

Molecular docking studies of disubstituted 1, 3, 5-triazine derivatives as dual enzyme inhibitors in *Mycobacterium tuberculosis*

¹Divya Menon, ²Supriya Mahajan

¹Research scholar, ²Former Professor of Pharmaceutical Chemistry,

¹Department of Pharmaceutical Chemistry,

¹C. U. Shah College of Pharmacy, S. N. D. T. Women's University, Sir Vithaldas Vidyavihar, Juhu Road, Santacruz (W) Mumbai-49, India.

Abstract : Tuberculosis is a highly infectious disease and poses a threat to the wellbeing of people. *Mycobacterium tuberculosis*, the causative agent of the disease, develops resistance to antitubercular drugs and has the ability to lie dormant in the host, reactivating when the host is immunocompromised. Since it is seen that *Mycobacterium tuberculosis* can develop resistance to a drug, which targets a single protein or enzymatic pathway with ease, molecules which can have multiple targets need to be designed and materialized. Here, we report the docking results and interaction of twenty-six disubstituted 1, 3, 5-triazine derivatives as dihydrofolate reductase (DHFR) and enoyl acyl carrier protein reductase (InhA) inhibitors.

IndexTerms - *Mycobacterium tuberculosis*, dual enzyme inhibitors, DHFR, InhA.

I. INTRODUCTION

Tuberculosis (TB) is a contagious disease and is one of the top ten causes of death worldwide. It primarily affects the lungs but it can affect other sites as well. It is caused by the bacillus, *Mycobacterium tuberculosis* (Mtb).^[1]

Multi-drug and extensively-drug resistant strains of TB are seen in the world today. Hence, it is of utmost importance to invest significant resources available to us in order to identify new drug entities that can tackle this disease effectively.

It should also be noted that other factors like appropriate nourishment of the patient, adherence to the drug regimen by the patient and good quality of drugs supplied for the patient, also play important role when it comes to the matter of tackling the disease effectively.

Dihydrofolate reductase (DHFR) is an enzyme, which catalyzes the reduction of dihydrofolate to tetrahydrofolate using NADPH as a cofactor. Tetrahydrofolate is essential for the synthesis of thymidylate, purines and amino acids. The inhibition of the enzyme would lead to disruption of DNA synthesis and consequent cell death.^{[2][3]}

A triazine DHFR inhibitor, WR99210, which was exhaustively studied against the malarial parasite *Plasmodium falciparum*, also showed activity against mycobacteria. Gerum *et al* screened 19 compounds related to WR99210, of which 7 showed potent Mtb DHFR inhibition. The screening of the compounds was done using an engineered strain of budding yeast, *Saccharomyces cerevisiae*, which was dependent on Mtb DHFR for its growth.^[4]

The crystal structure of Br-WR99210:NADP:DHFR complex was resolved, which revealed the conformation of Br-WR99210, which is a brominated analogue of WR99210 in the active site of the DHFR enzyme 1DG7, with a resolution of 1.8 Å.^[5]

Tawari *et al* have reported a series of 2, 4-diaminotriazines as Mtb DHFR inhibitors. Of the derivatives that they designed and synthesized, two compounds showed potent whole cell activity against Mtb H37Rv, low cytotoxicity against VERO cell lines and approximately 65 to 80 times more selectivity towards Mtb DHFR, when compared with the standard drug methotrexate.^[6]

Enoyl acyl carrier protein reductase (InhA) plays an important role in the biosynthesis of mycolic acid, which is an essential constituent of the cell wall of *Mycobacterium tuberculosis*. InhA catalyzes the NADH dependent reduction of enoyl acyl carrier protein (enoyl-ACP) to acyl-ACP in the final step of the Fatty Acid Synthase-II (FAS-II) pathway.^[7]

Isoniazid, which is a frontline antitubercular agent, is a prodrug which is converted to the active acyl radical form by the mycobacterial enzyme catalase-peroxidase (KatG). This active form of isoniazid forms an adduct with NAD⁺ to inhibit the enzyme. Resistance to the drug has developed because of mutation in the KatG enzyme. Hence, direct inhibitors of the enzyme, which need no prior activation, were synthesized and their InhA enzyme inhibitory activity studied.^[8]

Several 1, 2, 3-triazole derivatives, substituted with hydrophobic side chains, have been studied for their InhA enzyme inhibitory activity in both *in silico* and *in vitro* formats.^{[9][10]}

It can be hypothesized that 1, 3, 5-triazines, which show bioisosterism with 1, 2, 3-triazole moiety, can be linked with various hydrophobic substituents to elicit similar inhibition of the InhA enzyme.

Here, we report the *in silico* interaction of 26 disubstituted 1, 3, 5-triazine derivatives in both DHFR and InhA enzymes.

II. MATERIALS AND METHODS

2.1 Computational tools

For the *in silico* docking studies, *Maestro 11*, a Molecular Modeling Software from Schrödinger, was used. *Maestro* is the graphical user interface for nearly all of Schrödinger computational programs. It was installed on a computer system having Windows XP as an operating system and having a configuration of 3.4 GHz Pentium-4 processor with 1GB RAM and 160 GB Hard Disk.

The following steps were involved in the docking process:

2.1.1 Ligand preparation

The 2D structure of the ligand was drawn using the *build* panel on *Maestro*. This 2D structure was then run through the program *LigPrep* to generate the optimized 3D structure of the ligand. This optimized ligand was then used for docking. **Figure 1** represents the 3D structure of the ligand (compound C11), which was processed by using the program *LigPrep*.

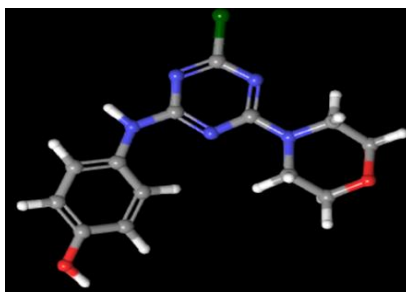


Figure 1: 3D structure of compound C11 obtained from *LigPrep*

2.1.2 Protein preparation

The X-ray crystallographic structures of both the enzymes DHFR and InhA were downloaded from Research Collaboratory for Structural Bioinformatics (RCSB) with PDB ID 1DG7 and 2NSD, respectively. The enzyme 1DG7 contains *Mycobacterium tuberculosis* dihydrofolate reductase (DHFR) complexed with NADPH and an in-built inhibitor Br-WR99210. It has a resolution of 1.8 Å. The enzyme 2NSD contains *Mycobacterium tuberculosis* enoyl acyl carrier protein reductase (InhA) complexed with NADH and an in-built inhibitor N-(4-methylbenzoyl)-4-benzylpiperidine (4PI). It has a resolution of 1.9 Å.

The raw enzymes were downloaded and processed using the program, *Protein Preparation Wizard*, to get the optimized protein which was used for docking. **Figure 2** depicts the raw and the optimized proteins 1DG7 and 2NSD.

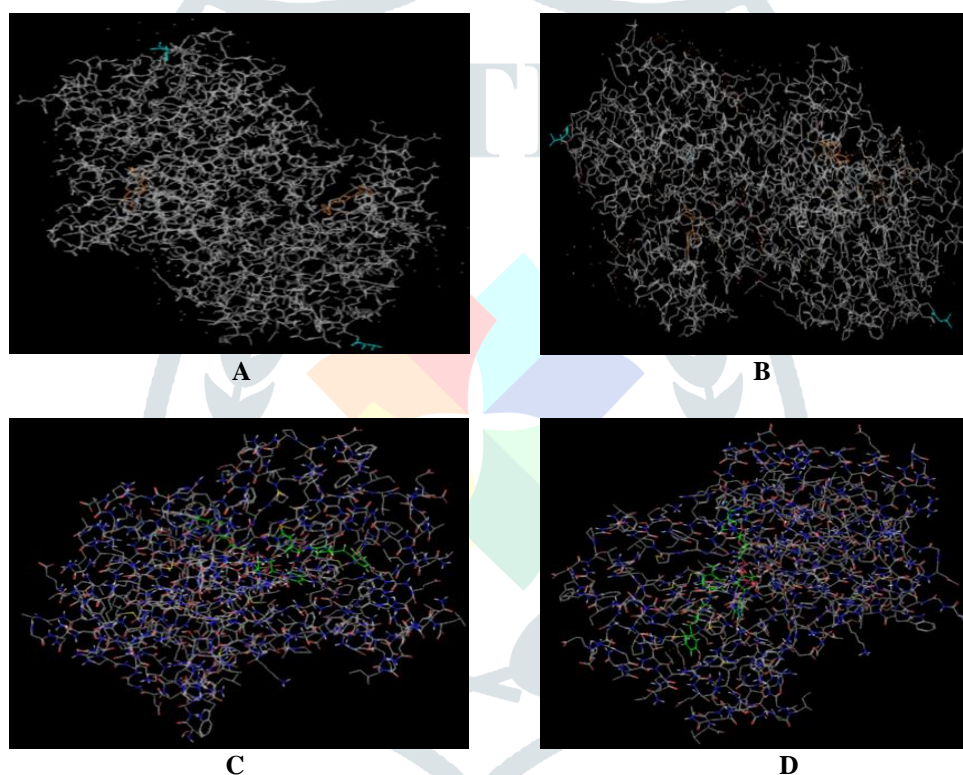


Figure 2: The images A and B represent the raw proteins of 1DG7 and 2NSD, respectively, downloaded from the Protein Data Bank. The images C and D represent the optimized proteins of 1DG7 and 2NSD, respectively, processed by *Protein Preparation Wizard*.

2.1.3 Grid generation

The receptor grid was generated in the active site of the enzyme by using the *Glide Receptor Grid Generation Wizard*. During the grid generation, the in-built inhibitor around which the grid box is generated, was selected. The in-built inhibitor was excluded from the receptor grid generation calculation. The size of the grid was adjusted. **Figure 3** represents the grid generated around the in-built inhibitors in the active site of the enzymes 1DG7 and 2NSD.

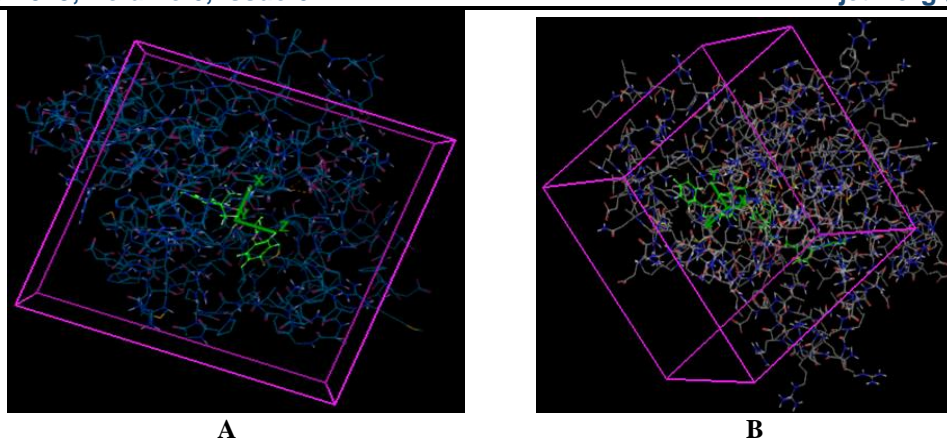


Figure 3: The image A shows the grid generated around the in-built inhibitor Br-WR99210 in the enzyme 1DG7 and image B shows the grid generated around the in-built inhibitor 4PI in the enzyme 2NSD.

2.1.4 Validation

The in-built inhibitors, Br-WR99210 and 4PI, in case of the enzymes 1DG7 and 2NSD, respectively, were split (de-docked) from the active site. It was then redocked onto the active site. The de-docked and redocked in-built inhibitors were superimposed. The Root Mean Square Deviation (RMSD) should be less than 1. **Figure 4** depicts the superimposed in-built inhibitor Br-WR99210 of the enzyme 1DG7 and the in-built inhibitor 4PI of the enzyme 2NSD.

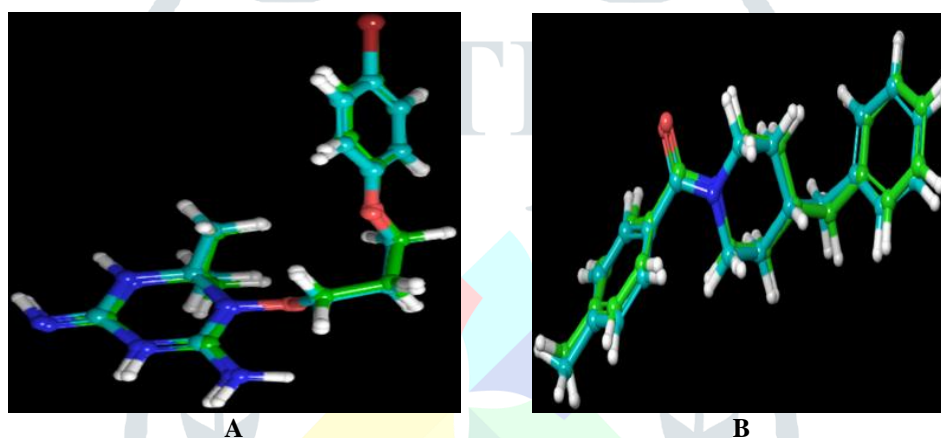
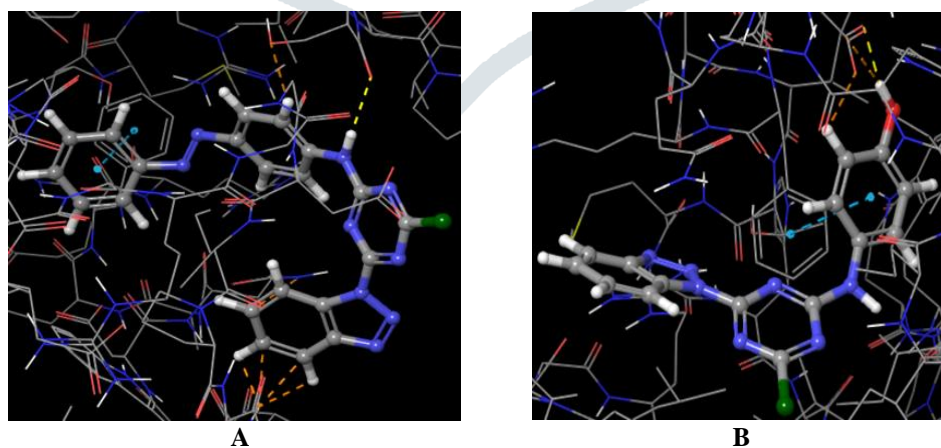


Figure 4: The image A depicts the superimposed in-built inhibitor Br-WR99210 of the enzyme 1DG7 and the image B depicts the superimposed in-built inhibitor 4PI of the enzyme 2NSD.

2.1.5 Docking

Docking study was performed using the program *Glide*. During docking, the ligand was flexible, whereas the enzyme was held rigid. The ligands were docked in the active site of the enzymes and the docking results were expressed as G-score. **Figure 5** depicts the compounds W12 and C12 docked in the active sites of the enzymes 1DG7 and 2NSD.



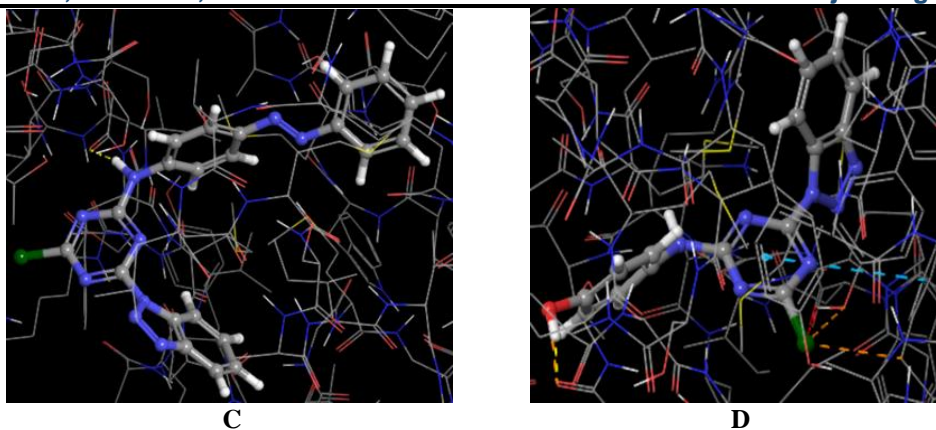


Figure 5: The images A and B depict the compounds W12 and C12 in the active site of the enzyme 1DG7 whereas the images C and D depict the compounds W12 and C12 in the active site of the enzyme 2NSD.

2.2 General structure of compounds

Thirteen compounds in the C and W series were designed with 1, 3, 5-triazine as the central moiety linked to substituents R₁ and p-aminophenol in case of compounds of C series and p-aminoazobenzene derivative in case of compounds of W series. Figure 6 depicts the general structure of the compounds in the C and W series. Table 1 gives the substituent R₁.

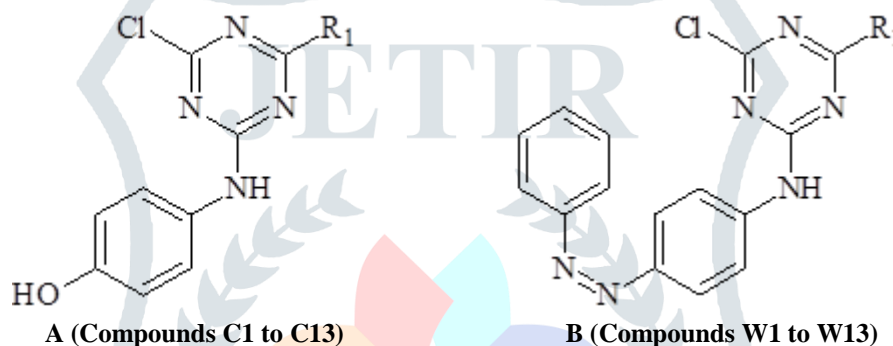

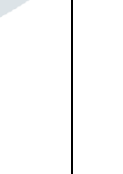



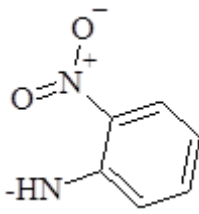
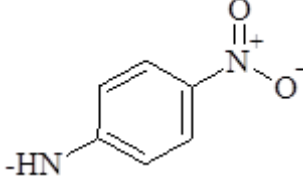
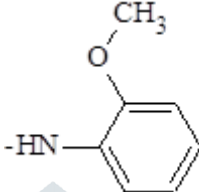
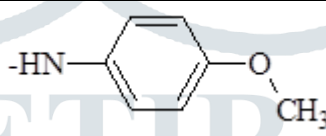
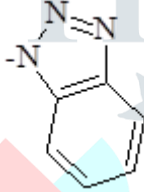





Figure 6: General structures of (A) compounds C1 to C13 and (B) compounds W1 to W13.

Table 1: Compound number and substituent present in compounds in C and W series

Compound number	Substituent (R ₁)
1	-HN- 
2	-HN- 
3	-HN- 
4	-HN- 
5	-HN- 

6	
7	
8	
9	
10	
11	
12	
13	

III. RESULTS AND DISCUSSION

3.1 Validation of the docking protocol

In case of the enzyme 1DG7, different grid sizes were generated and the RMSD values were determined for the purpose of validation. Table 2 gives various grid sizes that were generated around the in-built inhibitor Br-WR99210 at the active site of the enzyme 1DG7, along with the docking scores and the RMSD values.

Table 2: Various grid sizes, G-score and RMSD values for the in-built inhibitor Br-WR99210 of the enzyme 1DG7

Grid size (Å)	G-score (kcal/mol)	RMSD value
10	-6.38	2.73
13	-5.96	2.57
15	-6.11	2.83
17	-6.08	0.29
20	-5.69	2.62

Hence, Grid size of 17 Å was selected for docking the ligands since the RMSD value obtained was 0.2962, which was below 1.

In case of the enzyme 2NSD, different grid sizes were generated and the RMSD values were determined for the purpose of validation. Table 3 gives various grid sizes that were generated around the in-built inhibitor 4PI at the active site of the enzyme 2NSD along with the docking scores and the RMSD values.

Table 3: Various grid sizes, G-score and RMSD values for the in-built inhibitor 4PI of the enzyme 2NSD

Grid size (Å)	G-score (kcal/mol)	RMSD Value
10	-11.14	0.42
15	-11.56	0.45
20	-11.62	0.45

Here, the RMSD values observed was almost the same for all the grid sizes and hence, grid size of 20 Å was chosen because of highest G-score value.

3.2 Docking study

The disubstituted 1, 3, 5-triazine derivatives C1 to C13 and W1 to W13 were docked in the active site of the enzymes 1DG7 and 2NSD. On docking the ligands to the active site, the G-score was generated, which gave an idea about the binding affinity of the ligands to the active site of the enzyme. The interaction between the ligand and the important amino acid residues in the active site of the enzymes was studied.

Compounds C1 to C13 showed G-score ranging from -5.612 to -6.17 and compounds W1 to W13 showed G-score ranging from -4.603 to -6.257. The G-score of the in-built inhibitor Br-WR99210 for the enzyme 1DG7 was found to be -6.08. Compounds C1 to C13 showed G-score ranging from -6.799 to -9.957 and compounds W1 to W13 showed G-score ranging from -8.712 to -10.715. The G-score of the in-built inhibitor 4PI for the enzyme 2NSD was found to be -11.62.

Table 4 gives the G-score of the ligands C1 to C13, W1 to W13 and in-built inhibitor Br-WR99210 docked in the active site of the enzyme 1DG7 and Table 5 gives the G-score of the ligands C1 to C13, W1 to W13 and in-built inhibitor 4PI docked in the active site of the enzyme 2NSD.

Table 4: G-score of the ligands C1 to C13, W1 to W13 and in-built inhibitor Br-WR99210 docked in the active site of the enzyme 1DG7

Compound ID	G-score (kcal/mol)	Compound ID	G-score (kcal/mol)
C1	-5.63	W1	-4.956
C2	-5.687	W2	-5.163
C3	-5.681	W3	-5.321
C4	-5.708	W4	-4.944
C5	-5.626	W5	-6.257
C6	-5.924	W6	-5.978
C7	-5.967	W7	-4.603
C8	-5.935	W8	-5.373
C9	-5.612	W9	-5.809
C10	-6.087	W10	-5.627
C11	-6.17	W11	-4.965
C12	-5.969	W12	-5.065
C13	-5.749	W13	-5.358
Br-WR99210		-6.08	

Table 5: G-score of the ligands C1 to C13, W1 to W13 and in-built inhibitor 4PI docked in the active site of the enzyme 2NSD

Compound ID	G-score (kcal/mol)	Compound ID	G-score (kcal/mol)
C1	-8.161	W1	-9.195
C2	-8.237	W2	-10.698
C3	-9.957	W3	-10.601
C4	-6.799	W4	-8.949
C5	-9.078	W5	-9.194
C6	-9.151	W6	-9.106
C7	-7.905	W7	-10.664
C8	-8.884	W8	-9.038
C9	-7.794	W9	-10.446
C10	-9.74	W10	-10.715
C11	-8.274	W11	-8.712
C12	-8.166	W12	-9.938
C13	-7.954	W13	-9.947
4PI		-11.62	

3.3 Ligand interaction diagram

3.3.1 Interaction of compounds in the active site of the enzyme 1DG7

As observed in the literature, the in-built inhibitor Br-WR99210 interacts with several important amino acid residues in the active site of the enzyme 1DG7. The two amino groups of Br-WR99210 form hydrogen bonds (H-bonds) with the residues Ile5, Ile94 and Asp27. The bromide group forms a halogen bond with the residue Lys53. Apart from these interactions, other important amino acid residues such as Ala7, Ile20, Phe31, Thr46 and Leu50, mentioned in the literature, are also present in the active site of the enzyme.

The pink arrows in the ligand interaction diagram represent the H-bonds that the amino groups of the in-built inhibitor Br-WR99210 of the enzyme 1DG7 forms with the amino acid residues on the enzyme. **Figure 7** show the ligand interaction diagram of the in-built inhibitor Br-WR99210 in the active site of the enzyme 1DG7.

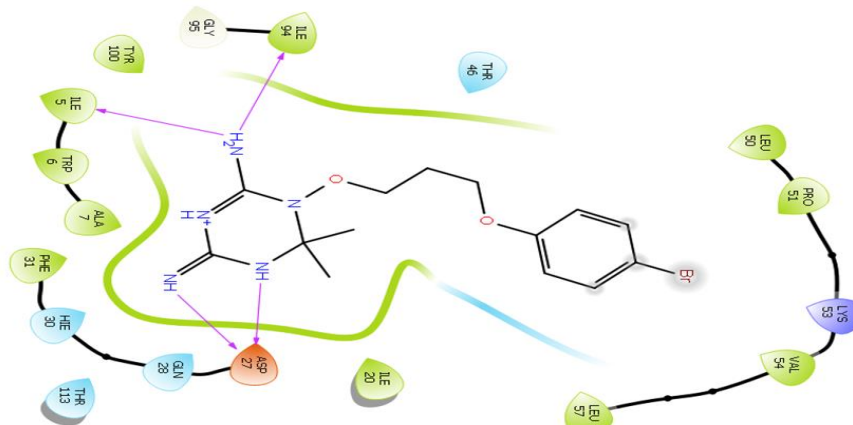


Figure 7: Ligand interaction diagram of an in-built inhibitor Br-WR99210 in the active site of the enzyme 1DG7

The docked ligands lack the 2, 4-diamino group that is present in the in-built inhibitor. Hence, the interaction of the docked ligands with amino acid residues are different from that observed for the in-built inhibitor.

The ligand interaction diagram of compound W13 in the active site of the enzyme 1DG7 is shown in **Fig.8**. It shows H-bond (pink arrow) formation with the residue Ile94, π - π stacking (green line) interaction with Phe31 and formation of π -cation (red line) with the residue Arg32. The analysis of the ligand interaction diagram of all the compounds in the W series showed that they formed π - π stacking interaction with Phe31, H-bond formation with residues Ser49, Gln28 and Ile20, halogen bond formation with the residue Ser49, π -cation formation with residues Arg32, Lys53 and Phe31 and salt bridge formation with Arg146.

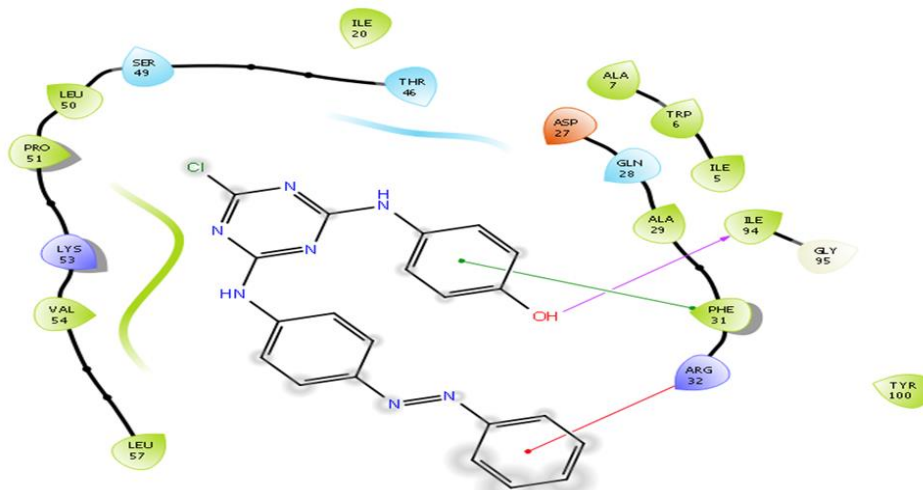


Figure 8: Ligand interaction diagram of compound W13 in the active site of the enzyme 1DG7

The ligand interaction diagram of compound C11 in the active site of the enzyme 1DG7 is shown in **Fig.9**. It shows that the compound forms H-bond with the residues Ile94 and Asp27 and also π - π stacking interaction with the residue Phe31. The analysis of the ligand interaction diagram of all the compounds in the C series showed that they formed π - π stacking interaction with Phe31, H-bond formation with Asp27, Trp22 and Lys53, halogen bond formation with Ser49, π -cation with Phe31 and salt bridge with Lys53.

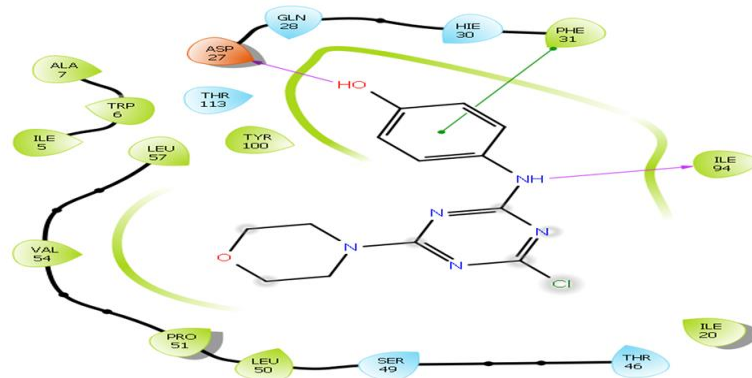


Figure 9: Ligand interaction diagram of compound C11 in the active site of the enzyme 1DG7

3.3.2 Interaction of compounds in the active site of the enzyme 2NSD

In accordance with the literature, the in-built inhibitor 4PI interacts with important amino acid residues present in the active site of the enzyme 2NSD. The amide carbonyl group oxygen of 4PI is H-bonded with Tyr158, which is considered as one of the catalytic residues in the InhA active site. The unsubstituted phenyl ring shows π - π stacking interaction with Phe149. The other important residues in the active site as given in the literature are Pro193, Val203, Leu218, Gly96. **Figure 10** shows the ligand interaction diagram of the in-built inhibitor 4PI in the active site of the enzyme 2NSD.

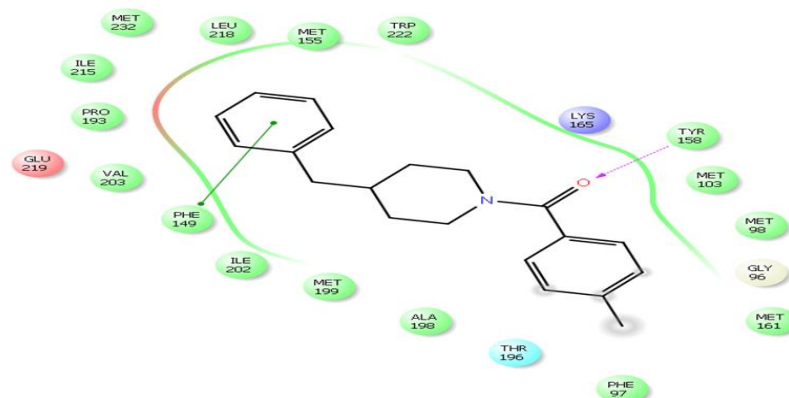


Figure 10: Ligand interaction diagram of an in-built inhibitor 4PI in the active site of the enzyme 2NSD

As seen in the ligand interaction diagram shown in **Fig.11**, the unsubstituted phenyl ring of the compound W8 exhibits π - π stacking interaction with Tyr158. On analyzing the ligand interaction diagram of the compounds in the W series, it was observed that all of them formed H-bond with Gly96. Compound W13 formed H-bond with Met103 apart from Gly96. Many compounds showed π - π stacking interaction with residues Tyr158, Phe97 and Phe149. Halogen bond formation was observed with the residue Met98.

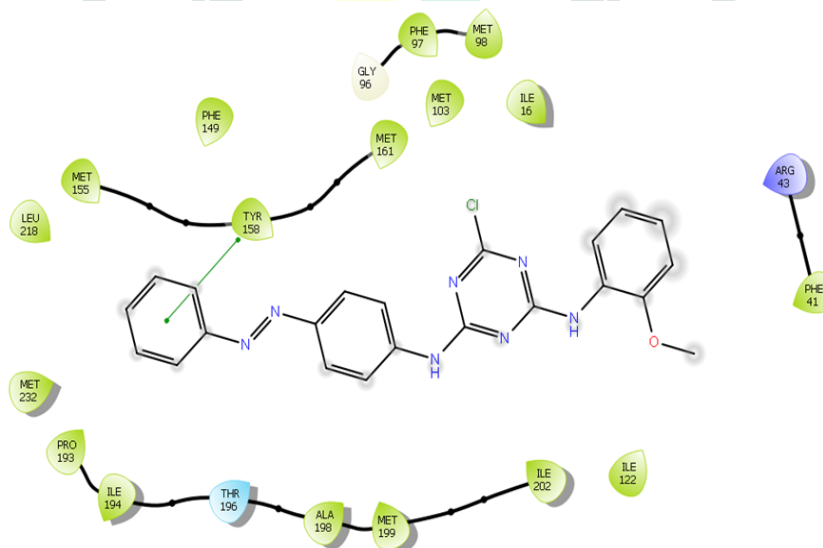


Figure 11: Ligand interaction diagram of compound W8 in the active site of the enzyme 2NSD

Figure 12 shows the ligand interaction diagram of compound C10, in the active site of the enzyme 2NSD. In the ligand interaction diagram of compound C10, it is seen that the 1, 3, 5-triazine ring exhibits π - π stacking interaction with Phe149 and hydroxyl group exhibits H-bond with the residue Gly96. On analyzing the ligand interaction diagram of the compounds in the C series, it was observed that they exhibit H-bond with the residues Gly96, Ile215 and Pro156. The compounds showed π - π stacking interactions with residues Tyr158 and Phe149. Halogen bond formation was observed with residues Tyr158 and Met98.

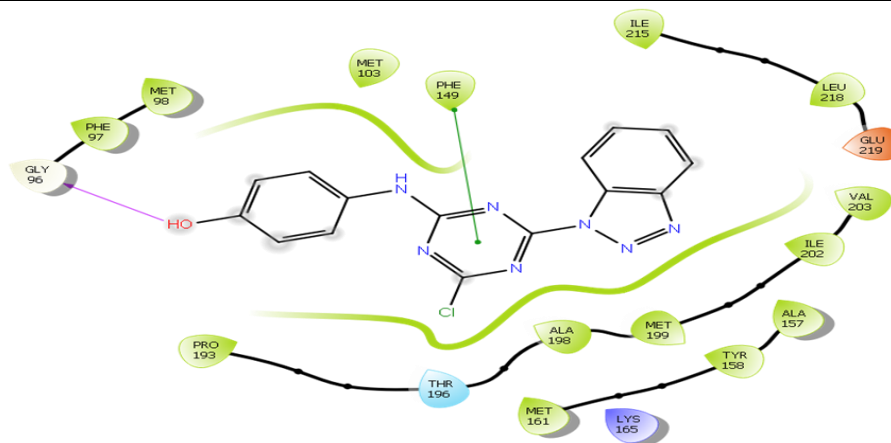


Figure 12: Ligand interaction diagram of compound C10 in the active site of the enzyme 2NSD

IV. CONCLUSION

The emergence of multi and extensively drug resistant forms of tuberculosis is a major cause of concern when it comes to the treatment of tuberculosis. *Mycobacterium tuberculosis* develops resistance to a drug by mutation in the enzyme targeted by the drug. Hence, it is important to develop compounds that can target multiple enzymes in the pathogen. Here we conducted an *in silico* docking study of twenty-six disubstituted 1, 3, 5-triazine derivatives as *Mycobacterium tuberculosis* DHFR and InhA enzyme inhibitors. It was seen that compounds C1 to C13 had G-scores in the range of -5.612 to -6.17 and -6.799 to -9.957, when docked in the enzymes 1DG7 and 2NSD, respectively. Compounds W1 to W13 had G-scores in the range of -4.603 to -6.257 and -8.712 to -10.715 in the enzymes 1DG7 and 2NSD, respectively. The interaction of the compounds in the active site of the enzymes was studied. The compounds interacted with the important amino acid residues in the active site of both the enzymes. These compounds will be synthesized and their antimycobacterial activity will be evaluated. Those compounds giving good minimum inhibitory concentration (MIC) in the screening assay against drug-susceptible and MDR-TB strains will be shortlisted to determine their enzyme inhibition activity via DHFR and InhA enzymes.

REFERENCES

- [1] WHO. 2019. Global Tuberculosis Report, accessed on 6th December 2019.
- [2] Gond, DS., Meshram, RJ., Jadhav, SG., Wadhwa, G., Gacche, RN. 2013. *In silico* screening of chalcone derivatives as potential inhibitors of dihydrofolate reductase: assessment using molecular docking, paired potential and molecular hydrophobic potential studies. *Drug Invention Today*, 5(3): 182-191.
- [3] Dias, MVB., Tyrakis, P., Domingues, RR., Leme, AFP., Blundell, TL. 2014. *Mycobacterium tuberculosis* dihydrofolate reductase reveals two conformational states and a possible low affinity mechanism to antifolate drugs. *Structures*, 22(1): 94-103.
- [4] Gerum, AB., Ulmer, JE., Jacobus, DP., Jensen, NP., Sherman, DR., Sibley, CH. 2002. Novel *Saccharomyces Cerevisiae* screen identifies WR99210 analogues that inhibit *Mycobacterium tuberculosis* dihydrofolate reductase. *Antimicrobial Agents and Chemotherapy*, 46(11): 3362-3369.
- [5] Li, R., Sirawaraporn, R., Chitnumsub, P., Sirawaraporn, W., Wooden, J., Athappilly, F., Turley, S., Hol, WGJ. 2000. Three-dimensional structure of *M. tuberculosis* dihydrofolate reductase reveals opportunities for the design of novel tuberculosis drugs. *Journal of Molecular Biology*, 295(2): 307-323.
- [6] Tawari, NR., Bag, S., Raju, A., Lele, AC., Bairwa, R., Ray, MK., Rajan, MGR., Nawale, LU., Sarkar, D., Degani, MS. 2015. Rational drug design, synthesis and biological evaluation of dihydrofolate reductase inhibitors as antituberculosis agents. *Future Medicinal Chemistry*, 7(8): 979-988.
- [7] Manjunatha, UH., Rao, SPS., Kondreddi, RR., Noble, CG., Camacho, LR., Tan, BH., Ng, SH., Ng, PS., Ma, NL., Lakshminarayana, SB., Herve, M., Barnes, SW., Yu, W., Kuhen, K., Blasco, F., Beer, D., Walker, JR., Tonge, PJ., Glynne, R., Smith, PW., Diagana, TT. 2015. Direct inhibitors of InhA active against *Mycobacterium tuberculosis*. *Scientific Translational Medicine*, 7(269): 269ra3.
- [8] He, X., Alian, A., Ortiz de Montellano, PR. 2007. Inhibition of *Mycobacterium tuberculosis* enoyl acyl carrier protein reductase InhA by arylamides. *Bioorganic and Medicinal Chemistry*, 15(21): 6649-6658.
- [9] Nalla, V., Shaikh, A., Bapat, S., Vyas, R., Karthikeyan, M., Yogeewari, P., Sriram, D., Muthukrishnan, M. 2018. Identification of potent chromone embedded [1,2,3]-triazoles as novel anti-tubercular agents. *Royal Society Open Science*, 5(4): 171750.
- [10] Ghiano, DG., Iglesia, A., Liu, N., Tonge, PJ., Morbidoni, HR., Labadie, GR. 2017. Antitubercular activity of 1,2,3-triazolyl fatty acid derivatives. *European Journal of Medicinal Chemistry*, 125: 842-852.